Review Article

Experiments on Linear and Nonlinear Localization of Optical Vortices in Optically Induced Photonic Lattices

Daohong Song,[1] Cibo Lou,[1] Liqin Tang,[1] Zhuoyi Ye,[1] Jingjun Xu,[1] and Zhigang Chen[1, 2]

[1] *The Key Laboratory of Weak-Light Nonlinear Photonics, Ministry of Education and TEDA Applied Physics School, Nankai University, Tianjin 300457, China*
[2] *Department of Physics & Astronomy, San Francisco State University, San Francisco, CA 94132, USA*

Correspondence should be addressed to Zhigang Chen, biglasers@gmail.com

We provide a brief overview on our recent experimental work on linear and nonlinear localization of singly charged vortices (SCVs) and doubly charged vortices (DCVs) in two-dimensional optically induced photonic lattices. In the nonlinear case, vortex propagation at the lattice surface as well as inside the uniform square-shaped photonic lattices is considered. It is shown that, apart from the fundamental (semi-infinite gap) discrete vortex solitons demonstrated earlier, the SCVs can self-trap into stable gap vortex solitons under the normal four-site excitation with a self-defocusing nonlinearity, while the DCVs can be stable only under an eight-site excitation inside the photonic lattices. Moreover, the SCVs can also turn into stable surface vortex solitons under the four-site excitation at the surface of a semi-infinite photonics lattice with a self-focusing nonlinearity. In the linear case, bandgap guidance of both SCVs and DCVs in photonic lattices with a tunable negative defect is investigated. It is found that the SCVs can be guided at the negative defect as linear vortex defect modes, while the DCVs tend to turn into quadrupole-like defect modes provided that the defect strength is not too strong.

1. Introduction

Vortices and vortex solitons are ubiquitous in many branches of sciences such as hydrodynamics, superfluid, high-energy physics, laser and optical systems, and Bose-Einstein condensates [1, 2]. In optics, optical vortices are phase singularities embedded in electromagnetic waves, and the intensity in a singularity point vanishes due to the undetermined phase. The field phase changes by $2\pi m$ (m is an integer called topological charge) along any closed loop around the singularity point. The study of linear and nonlinear propagation dynamics of optical vortex beams in continuum media attracted great attentions for decades [1]. In general, a vortex dark ring beam will expand during linear propagation due to the diffraction. However, nonlinearity can compensate the diffraction, leading to the formation of nonlinear localized states called spatial vortex solitons. It is found that an optical vortex can self-trap into a vortex soliton in nonlinear media with a *self-defocusing* nonlinearity [3–7], even the vortex is nested in a partially incoherent optical beam [8]. However,

with a *self-focusing* nonlinearity, optical vortices tend to breakup into filaments due to the azimuthally modulation instabilities [9].

Several different physical mechanisms have been proposed for suppression of the azimuthally instability [10–12]. Guiding the vortices in periodic structures such as photonic crystals or photonic lattices opened a new avenue to stabilize optical vortices in nonlinear media. Generally speaking, the vortices propagation in periodic structures is dominated by the lattice discreteness, nonlinearity, and the phase singularity. Therefore, the localization and stabilization of such vortices exhibit many new phenomena which do not exist in continuous medium. In fact, discrete SCV solitons have been both theoretically predicated and successfully observed experimentally in square photonic lattices with self-focusing nonlinearity under four-site excitation [13–16]. Singly charged high-band vortex solitons are also realized in photonic lattices [17]. On the other hand, DCV propagation in isotropic square photonic lattice leads to periodic charge flipping with a quadrupole-like mediate states [18].

Stable SCV, DCV, and multivortex solitons in hexagonal lattices have also been experimentally demonstrated [19–21]. Besides square-like and hexagonal lattices, it has also been proposed that discrete vortex solitons with higher topological charges even exist in photonic quasicrystals [22].

In this paper, we present a brief overview of our recent work on both linear and nonlinear propagation of SCV and DCV beams in 2D photonic lattices in bulk photorefractive material by optical induction. In the nonlinear cases, vortex beam propagation both inside and at the surface of photonic lattices is considered. We show that under appropriate nonlinear conditions both SCV and DCV beams can stably self-trapped into a gap vortex soliton in photonic lattices with self-defocusing nonlinearity. While a SCV beam can turn into a stable gap vortex soliton under four-site excitation, a DCV beam tends to turn into a quadrupole gap soliton which bifurcates from the band edge. However, under geometrically extended eight-site excitation, the DCV can evolve into a stable gap vortex soliton. At the interface between photonics lattice and a homogenous media, under appropriate conditions, the SCV beam can turn into a stable surface discrete vortex soliton under four-site excitation with self-focusing nonlinearity, while it self-traps into a quasi-localized surface state under single site excitation. The stability of such nonlinear localized states is monitored by the numerical simulation to long propagation distance. In the linear case, the SCV beam can also evolve into a linear localized vortex defect mode in photonic lattice with a negative defect, while the DCV beam turns again into a quadrupole-like defect mode, provided that the defect strength is not too deep. Our results may prove to be relevant to the studies of similar phenomena in superfluids and Bose-Einstein condensates.

2. Experimental Setup

The experimental setup for our study is similar to those we used earlier for observation of discrete solitons [15, 23, 24], as shown in Figure 1, except that the input probe beam here can be either a SCV or DCV beam. Our experiments are typically performed in a biased SBN : 60 ($5 \times 5 \times 10 \text{ mm}^3$) photorefractive crystal illuminated by a laser beam with wavelength 488 nm from the Argon ion lasers. The biased crystal provides a self-focusing or defocusing non-instantaneous nonlinearity by simply reversing the external biased field. To generate a 2D-waveguide lattice, we use an amplitude mask to spatially modulate the otherwise uniform incoherent beam after the diffuser. The rotating diffuser turns the laser beam into a partially spatially incoherent beam with a controllable degree of spatial coherence. The mask is then imaged onto the input face of the crystal; the periodic intensity pattern is a nearly nondiffracting pattern throughout the crystal after proper spatial filtering. The lattice beam is ordinarily polarized, so it will induce a nearly linear waveguide array that remains invariant during propagation. We can create not only uniform lattices but also lattices with negative defects and lattices with sharp surfaces by simply changing the specially designed amplitude

mask. The extraordinarily polarized beam passes through a computer generated hologram to create a ring vortex beam, and then it is focused by a circular lens. The vortex beam is then used as our probe beam or *soliton-forming* beam, propagating collinearly with the *lattice-inducing* beam. In our experiment, the linear propagation of the vortex beam can be realized either by keeping the vortex beam at low intensity or by taking advantage of the noninstantaneous of the photorefractive nonlinearity. A weak reference beam is introduced to interfere with the vortex probe beam after it exits the crystal (bottom path of the Figure 1).

A piezotransduced (PZT) mirror is added to the optical path of the reference beam which can be used to actively vary the relative phase between the plane wave and the vortex beam. In addition, a white-light background beam illuminating from the top of the crystal is typically used for fine-tuning the photorefractive nonlinearity [8, 15].

3. Nonlinear Localization of Optical Vortices in Photonic Lattices

3.1. Discrete Gap Vortex Solitons. First, we study the SCV and DCV beams propagating inside optically induced photonic lattices under the self-defocusing nonlinearity. We find that a donut-shaped SCV beam can self-trap into a stable gap vortex soliton, while the DCV beam evolves into a quadruple soliton under the four-site excitation. Spectrum measurement and numerical analysis suggest that the gap vortex soliton does not bifurcate from the edge of the Bloch band, quite different from previously observed spatial gap solitons.

In our experiment, the lattice beam induces a "backbone" lattice with a self-defocusing nonlinearity where an intensity minimum corresponds to an index maximum [25]. The off-site excitation scheme is used so that the vortex core is on an index minimum, while the donut-like vortex beam covers four adjacent index maxima. Under proper conditions, self-trapping of the vortex beam can be established. Typical experimental results are presented in Figure 2, for which the lattice spacing is about 27μm, the intensity ratio of the vortex beam to the lattice beam is about 1 : 4, and the bias field is about -1.2 kV/cm. The interferograms of the input vortex beam with an inclined plane wave are shown in Figure 2, where the central fork in the interference fringes indicates the phase singularity ($m = 1$ for top panels and $m = 2$ for bottom panels) of the vortex beam. When the self-trapped state is established in the nonlinear regime, both $m = 1$ and $m = 2$ vortices break up into four filaments to cover the initially excited four lattice sites, just as in the self-focusing case [15, 16] except with longer tails along the two principal axes. Although the intensity patterns of self-trapped $m = 1$ and $m = 2$ vortices look somewhat similar, significant differences can be found in their phase structure and spatial spectrum. Two different interference techniques are used to identify the phase structure of self-trapped vortices. One is to send a titled broad beam (quasiplane wave) to interfere with the output vortex beam (Figure 2(c)). For the limited propagation distance of our crystal length
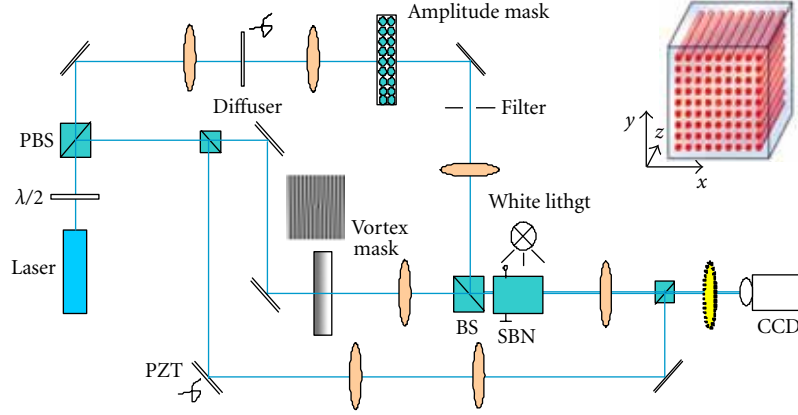
FIGURE 1: Experimental setup for optical induction of photonic lattices in a biased photorefractive crystal by amplitude modulation of a partially coherent beam. PBS: polarizing beam splitter; SBN: strontium barium niobate. Top path is the lattice-inducing beam, the middle path is the probing vortex beam, and the bottom path is the reference beam. The top right insert illustrates the scheme of induced waveguide arrays in the otherwise uniform SBN nonlinear crystal.

(10 mm), it appears that the vortex singularity (manifested by the central forks in the interferograms) persists after the nonlinear propagation through the crystal, although it seems that charge-flipping (reversal of forks) is associated with the DCV at crystal output. However, from numerical simulations to longer propagation distances, the singularity can maintain only for the $m = 1$ but not for the $m = 2$ vortices [26]. In fact, our theoretical analysis shows that a "true" doubly charged gap vortex soliton does not exist under this excitation condition, and a quadrupole-like soliton structure is found instead for the $m = 2$ vortex [26]. The other technique is to send a coaxial broad Gaussian beam as an interference beam. We can clearly see that the phase structure for self-trapped $m = 1$ and $m = 2$ vortices is different (Figure 2(d)). The two diagonal spots are out-of-phase for the $m = 1$ vortex but in-phase for the $m = 2$ vortex.

We also measure the spatial spectrum of self-trapped vortices by using the Brillouin Zone (BZ) Spectroscopy technique [27]. Again, dramatic difference between $m = 1$ and $m = 2$ vortices can be seen in the k-space spectra, indicating quite different physical pictures for self-trapping. For the $m = 1$ vortex, most of the power is located alongside the first BZ, but it would not concentrate just to the four corner points (corresponding to four high-symmetry M points) which mark the edge of the first Bloch band and where the diffraction is anomalous. However, for the $m = 2$ vortex, the nonlinear spectrum reshaping makes the power spectrum settle into the M-points quickly, similar to those of the fundamental discrete gap solitons and gap soliton trains [28]. Numerical simulations show that such spectrum difference remains for long propagation distance. These results suggest that although the $m = 1$ vortex can evolve into a gap vortex soliton, it does not bifurcate from the edge of the first Bloch band, quite different from all previously observed fundamental, dipole, or quadrupole-like gap soliton in self-defocusing lattices [28, 29]. On the other hand, the $m = 2$ vortex can evolve into a quadrupole-like localized state, which does seem to bifurcate from the edge

of the first Bloch bands as confirmed by numerical analysis [26, 30].

The experimental observations are also compared with the numerical results obtained using beam propagation method with initial conditions similar to that for the experiment. The numerical model is a nonlinear wave equation with a 2D square lattice potential under saturate self-defocusing nonlinearity. Excellent agreement can be found for the propagation distance of 10 mm (i.e., our crystal length) for both $m = 1$ and $m = 2$ vortices [26]. To test whether the relevant gap soliton structure can persist for longer propagation distance, simulations are performed with propagation distance up to 40 mm while all other parameters are unchanged. It is found that the phase singularity can maintain for the singly charged vortex, while for the doubly charged vortex at long propagation distance, it turns into a quadrupole-like structures. The simulation results are shown in Figure 3. Notice that the interference patterns of the nonlinear output with a tilted plane wave show that the fork is still in the center for the $m = 1$ vortex, but this is not the case for the $m = 2$ vortex which turns into an out-of-phase quadrupole soliton. The power spectrum is also similar to that of 1 cm propagation in experiment: the spectrum for the $m = 1$ gap vortex soliton does not evolve into the vicinity of the first-band M points, whereas that for the $m = 2$ vortex does. Intuitively, the nonedge bifurcation of the singly charged gap vortex may be attributed to the nontrivial helical phase structure of the vortex, which cannot be expressed as a simple superposition of linear Bloch modes near the band edge. Such subtle difference between the SCV and DCV gap solitons is also confirmed by theoretical analysis [26].

It is interesting to explore whether stable doubly charged gap vortex soliton exists in *self-defocusing* square photonic lattices without "decaying" into a quadrupole soliton, although such stable high-order discrete vortex solitons have been observed in hexagonal photonic lattices under a *self-focusing* nonlinearity [20]. Indeed, we find that when the input vortex ring is expanded to cover eight lattice

sites as shown in Figure 4(a), under appropriate nonlinear conditions, the phase singularity can maintain and it can evolve into a "true" stable gap vortex soliton. Typical experimental results are shown in Figure 4, where the results were obtained when the lattice spacing is 25 μm, the intensity ratio of the vortex beam to the lattice beam is 1 : 4, and the bias field is -1.4 kV/cm. When the nonlinear self-trapped state is realized, most of its energy is localized in the initially excited eight lattices (Figure 4(c)). More importantly, the interference pattern between an inclined plane wave and the nonlinear output clearly shows that the two forks along with the bifurcation direction still preserve compared with those of the input vortex shown in Figure 4(b). Again, in such a case, the spectrum is not located in the four M points, different from the nonlinear spectrum under four-site excitation shown in Figure 2(e). Such high-order vortex gap solitons do not bifurcate from the band edge either! We want to mention that the DCV beams can also stably self-trap into solitons in the semi-infinite gap under self-focusing nonlinearity with 8-site excitation. Such geometrical extended stabilization mechanism has also been confirmed by theoretical analysis [31].

3.2. Discrete Surface Vortex Solitons. Discrete surface solitons form an important family of discrete solitons that exist at interface between the semi-infinite photonic lattices and a homogenous media [32]. Now, let us use the SCV beam to excite at the surface of the photonic lattice rather than inside the lattice under the self-focusing nonlinearity. Surface vortex solitons have also been theoretically considered [33, 34]. Here, we present our experimental results of discrete surface vortex solitons with different excitation conditions. Both single-site and four-site excitation schemes are considered. We find that a SCV beam under the four-site excitation can evolve into a stable discrete surface vortex soliton in the semi-infinite gap, while under the single-site excitation, it evolves into a unstable quasilocalized surface state in the first photonic bandgap. The stability of such localized surface states depending on their initial excitation has been studied numerically for longer propagation distance [35].

First, we use the single-site excitation so the vortex ring covers only one lattice site at the surface (Figure 5(a) top). The vortex beam exhibits asymmetric discrete diffraction when its intensity is low but self-traps at the surface site when its intensity is high while keeping the bias field (2.2 kV/cm) unchanged. Typical experimental results are present in Figure 5. The lattice spacing is about 30 μm. When the nonlinearity is absent (the intensity ration of vortex-to-lattice is less than 1 : 10), the vortex beam diffracts as shown in Figure 5(b). The diffraction tails have double peak intensity at each lattice site, indicating the excitation of second-band Bloch modes. The tail going into the lattice is much longer than that at the lattice surface, owing to surface enhanced reflection [36, 37]. As we increase the intensity ratio to 1 : 3, self-trapping of the vortex at the lattice surface occurs when the vortex confines more at the initial excitation site, maintaining a donut-shaped pattern (Figure 5(c) top). To verify its phase singularity, a tilted plane wave is introduced to interfere with the surface vortex beam. The single fork remains in the interferogram, indicating that the phase singularity is preserved during the 1 cm experimental propagation length. Since the input vortex beam is tightly focused, its initial k-space spectrum extends beyond the first BZ (Figure 5(e) top). Such input condition excites high-band Bloch modes. In the case of the self-focusing nonlinearity, this leads to that the power spectrum is concentrated at the normal diffraction regions outside the first BZ but close to the high-symmetry X-points, as shown in Figure 5(e) top. Apparently, such self-trapped surface vortex states arise from excitation of Bloch modes near the X-points of the second Bloch band. However, numerical results to longer propagation distance (4 cm) shows that these quasilocalized surface states residing in the first photonic bandgap are unstable and thus would break up after long-distance propagation [35].

Next, we use the four-site excitation so the vortex ring is expanded to cover four nearest lattice sites at the surface (the vortex core locates in the index minimum as off-site excitation, as shown in Figure 5(a) bottom). Under appropriate nonlinear conditions, the SCV self-traps into a discrete surface vortex soliton. Typical experimental results are presented in the bottom panels of Figure 5. At a low nonlinearity, the vortex beam exhibits discrete diffraction (Figure 5(b)). Notice that in this case, the diffracted intensity pattern does not have fine features of double-peak in each lattice site, different from that of single-site excitation. This suggests that, under this condition, the expanded vortex excites the first-band Bloch modes. At a high nonlinearity, self-trapping of the vortex beam into a four-spot pattern is achieved (Figure 5(c)).

Due to that the induced surface is slightly deformed, the four-spot does not match a perfect square pattern. To monitor the phase structure of the self-trapped vortex, an inclined plane wave is again introduced for interference. The vortex singularity persists clearly in the nonlinear output (Figure 5(d) bottom). The nonlinear spectrum is also different from that of single-site excitation shown in Figure 5(e), since now most of the energy is concentrated in the central region of the normal diffraction within the first BZ. This indicates that the surface vortex soliton is formed in the semi-infinite gap with modes primarily from near the Γ-point of the first Bloch band. As shown below, this four-site surface vortex soliton can be stable and thus remains invariant for long distance propagation.

Experimentally, it is difficult to test the stability of the self-trapped surface vortex structures due to the limited crystal length (i.e., 1 cm). Thus, we study the stability of the self-trapped vortex states by numerical simulation with parameters similar to the experimental conditions, but to much longer propagation distance (4 cm). For the four-site excitation vortex in the semi-infinite gap is stable, but for the single-site vortex in the Bragg reflection gap is unstable as shown in Figure 6. The nonlinear output of the SCV under single-site excitation broke up after 4 cm propagation, while the four-site surface soliton is nearly invariant. This stability analysis is also confirmed theoretically [35].
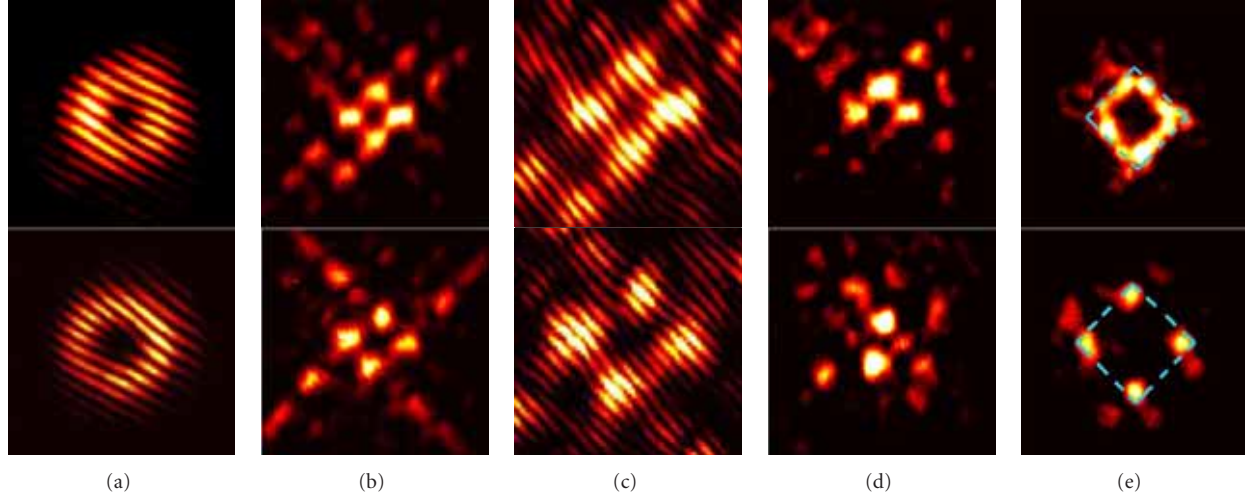
FIGURE 2: Experimental results of self-trapping of SCVs (top) and DCVs (bottom) in a defocusing photonic lattice. (a) Interferograms showing the phase of the input vortex beams, (b) intensity patterns of self-trapped vortex beams at lattice output, (c, d) interferograms between (b) and a tilted plane wave (c) and an on-axis Gaussian beam (d), respectively, and (e) the k-space spectra of (b) where the dash squares mark the first Brillouin zone of the square lattice. (a, c) are zoomed in with respect to (b, d) for better visualization.
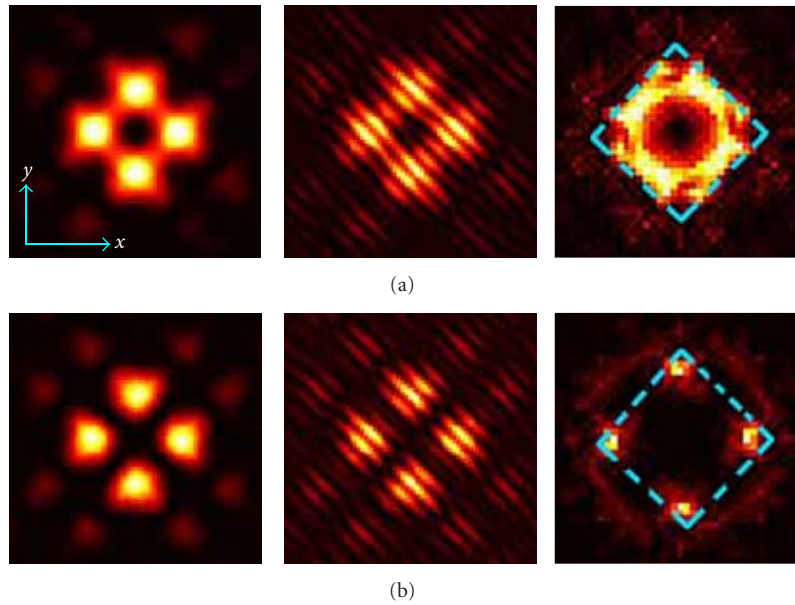

FIGURE 3: Simulation results of singly charged (a) and doubly charged (b) vortex beams propagating to a longer distance of 40 mm. Shown are the output transverse (x-y) intensity patterns (left), its interferogram with a tilted plane wave (middle), and its k-space spectrum (right) in both (a) and (b). Notice that the vortex singularity maintains in (a) but disappears in (b).

4. Linear Localization of Optical Vortices in Photonic Lattices with Negative Defects

In the previous experiments, the localization of the vortex beam inside and at the surface of the photonic lattice is related to the nonlinearity-induced defect by the vortex beam itself. These self-trapped nonlinear localized topological states can be considered as self-induced *nonlinear* defect modes (DMs). A nature question arises whether vortices can be localized in a fabricated defect as *linear* defect modes within photonic lattices? In fact, band gap guidance of a

Gaussian beam in photonic lattice with a negative defect has been realized in optically induced and fs-laser written waveguide arrays [38, 39].

Different from light guided in higher refractive-index region due to the total internal reflection, light guidance in negative defects results from the Bragg reflection in periodic structures. Here, we show that both a SCV and DCV beams can be guided in the negative defects in 2D photonic lattices provided the defect strength is not too deep. The experimental setup is similar to Figure 1, except that

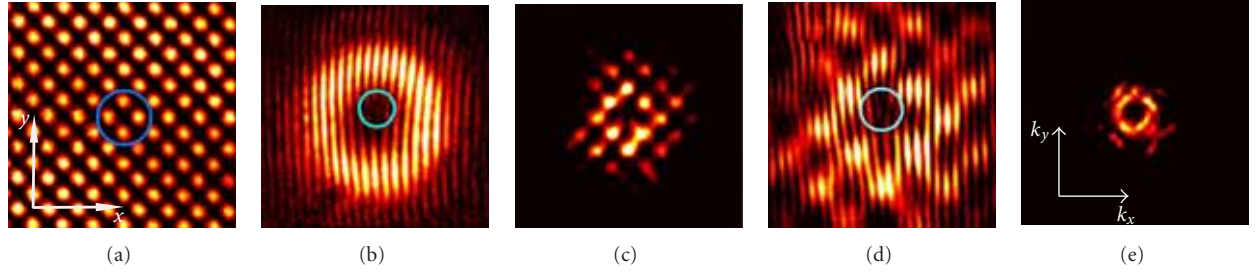(a)   (b)   (c)   (d)   (e)

FIGURE 4: Experimental observation of an extended $m = 2$ gap vortex soliton in photonic lattices with self-defocusing nonlinearity. (a) lattice beam, where the circle shows the location of the input vortex, (b) the interferogram of the input vortex with a tilted plane wave to show the phase singularity, (c) self-trapped vortex pattern, (d) the zoom-in interferogram of (c) with a tilted plane wave, and (e) the Fourier-space spectrum of the $m = 2$ vortex soliton. The circles in (b) and (d) show the position of the phase singularity.

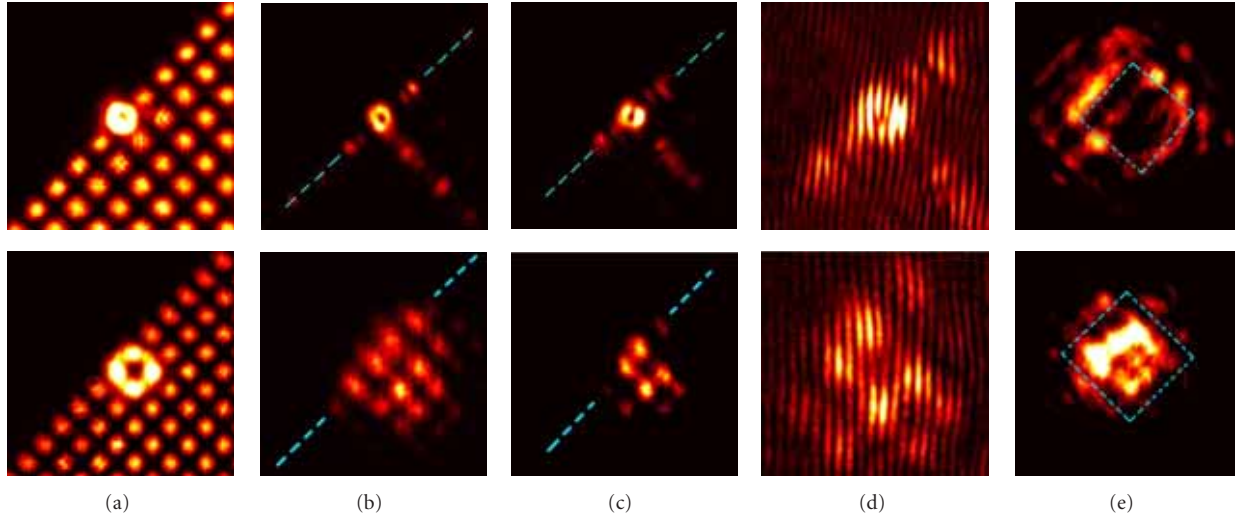(a)   (b)   (c)   (d)   (e)

FIGURE 5: Experimental results of vortex self-trapping under single-site surface excitation (top) and four-site surface excitation (bottom). (a) Lattice beam superimposed with the vortex beam, (b) linear and (c) nonlinear output of the vortex beam, where blue dashed line indicates the surface location, (d) zoom-in interferogram of (c) with an inclined plane wave, and (e) k-space spectrum of (c). The dashed square in (e) marks the boundary of the first Brillouin zone.

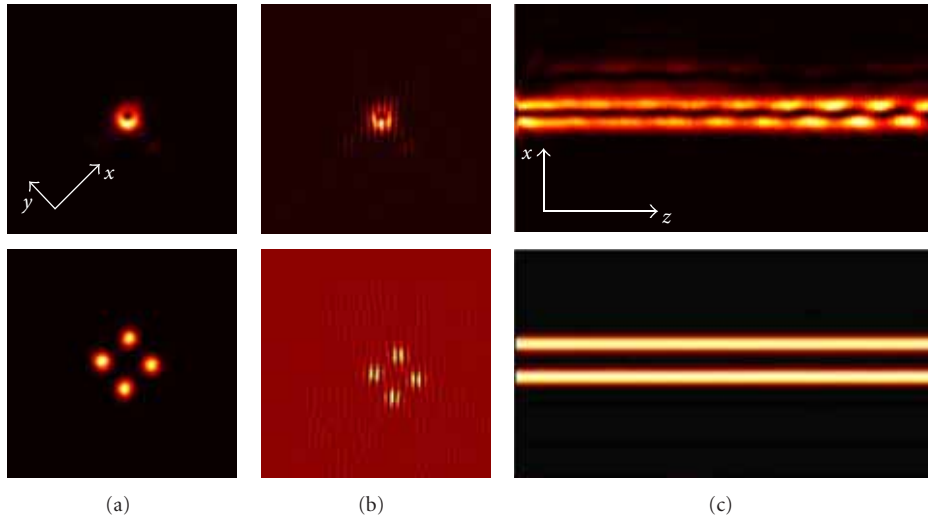

(a)   (b)   (c)

FIGURE 6: Numerical simulation of single-site (top) and four-site (bottom) surface excitation of a SCV after 4-cm of nonlinear propagation. Shown are (a) vortex output intensity pattern and (b) its corresponding interferogram, and (c) side-view of the vortex propagation to $z = 4$ cm.
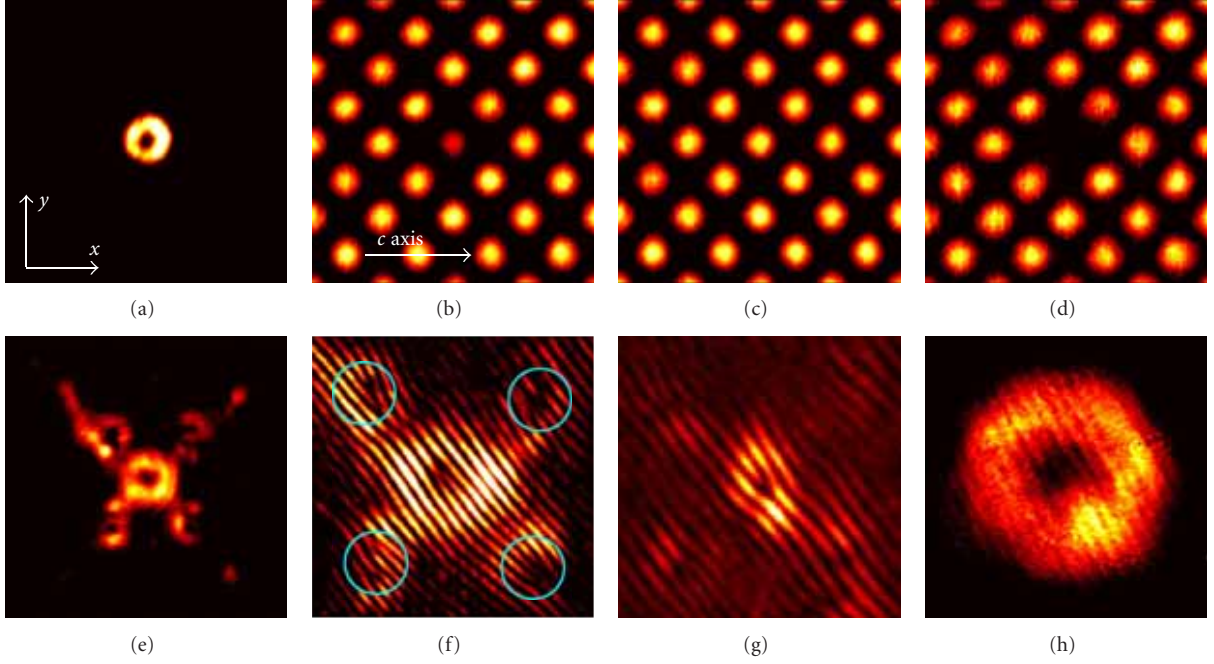
FIGURE 7: Experimental results of bandgap guidance of a vortex beam in a tunable negative defect. (a) Vortex at input. (b)–(d) Induced lattices with nonzero-intensity defect, no defect, and zero-intensity defect, respectively. (e), (f) Vortex output from the defect in (b) and its zoom-in interferogram. The circles in (f) mark the location of the vortex pairs. (g) Interferogram when the vortex is excited at nondefect site. (h) Vortex diffraction output when lattice is absent.
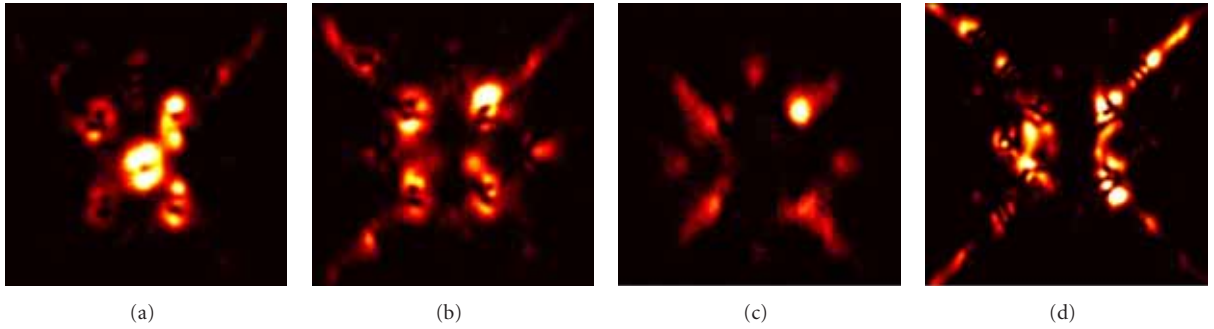

FIGURE 8: Experimental results of SCV beam output after propagating through (a) a half-intensity ($I_d/I_c = 1/1$) defect and (b) a zero-intensity defect at a fixed bias field of 2.6 kV/cm. (c), (d) Output of the vortex beam through the zero-intensity defect when the bias field is decreased to 1.4 kV/cm and increased to 3.2 kV/cm, respectively.
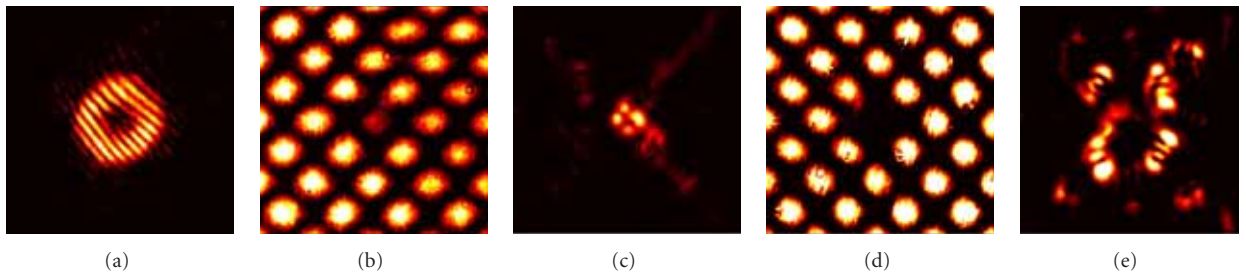

FIGURE 9: Experimental results of bandgap guidance f a DCV beam in a tunable negative defect. (a) interference pattern of input vortex with an inclined plane wave (zoomed in), (b) lattice beam with a nonzero-intensity defect, (c) linear output of the doubly charged vortex beam exiting the defect channel in the lattice (b), (d) lattice beam with a zero-intensity defect, and (e) linear output of the DCV through the defect in lattice (d).

the ordinarily-polarized beam is split again into two lattice-inducing beams: one has an uniform periodic intensity pattern as shown in Figure 7(c) (peak intensity I_c), and the other has a zero-intensity defect site on otherwise uniform periodic pattern as shown in Figure 7(d) [peak intensity I_d]. Superimposing the two lattice-inducing beams of equal lattice spacing results in a nonzero but tunable defect [an example obtained at $I_d/I_c = 1/2$ is shown in Figure 7(b)]. The tunability of the defect strength is realized by varying the intensity ratio I_d/I_c (e.g., at $I_d/I_c \gg 1$, the defect is deep or close to zero intensity, but at $I_d/I_c \ll 1$, the defect is shallow or close to washout).

Typical experimental results are presented in the bottom panels of Figure 7. Under proper experimental conditions, the input vortex beam (20 μm in diameter) is guided into the defect channel, maintaining a donut-shaped pattern in the defect site with "tails" extending along two principal axes of the square lattice. This result was obtained at 42 μm lattice spacing, 2.3 kV/cm, and $I_d/I_c = 1/2$. For comparison, the same vortex beam diffracts dramatically when the defect is removed, showing no self-action of the vortex beam under the same bias condition (Figure 7(h)). Fine features can be seen in the interferogram obtained by interference between the output vortex beam and an inclined broad beam (quasiplane wave). While the phase singularity is maintained in the vortex center, additional vortex pairs are evident along the four "tails" away from the defect site, manifested by two close but separated fork fringes in the interferogram (Figure 7(f)). These fine structures in the "tails" provide us a way to identify the properties of the vortex DMs. By comparing with the theoretical results [40], it is apparent that the input SCV beam has evolved into a high-gap DM, whose propagation constant resides between the second and third Bloch bands. We emphasize that the localization of the vortex beam arises from the linear bandgap guidance, quite different from stationary propagation of second-band vortex solitons where the vortex beam itself creates a positive defect with self-focusing nonlinearity [17]. For comparison, the interferogram from the vortex beam exiting a normal lattice site is shown in Figure 7(g), where a single vortex (instead of vortex pair) is observed along each "tail".

The formation of the vortex DMs depends on the defect strength. A series of experiments is performed to illustrate the influence of the defect strength. To do so, we keep the bias field and I_c fixed but tune the defect strength by gradually varying I_d. We found that the vortex can be guided only when the defect is not too deep (or the intensity in the defect site is not close to zero). Examples of varying the intensity ratio I_d/I_c or the bias field (both control the induced index change at the defect site) are shown in Figure 8. When the biased field is set at 2.6 kV/cm, guidance of the vortex beam is clearly observed at $I_d/I_c = 1$ (Figure 8(a)) (which corresponds to a half-intensity defect). However, once the uniform lattice beam is removed ($I_c = 0$), the vortex beam cannot be confined in the defect site under the same bias condition (Figure 8(b)). At this zero-intensity defect, the vortex DM cannot form, even at a decreased bias field of 1.4 kV/cm (Figure 8(c)) or an increased bias field of 3.2 kV/cm (Figure 8(d)). Thus, bandgap guidance

of the vortex clearly occurs in the half-intensity defect but deteriorates in the zero-intensity defect. There might be a threshold for the defect strength that would support the vortex DM, but experimentally it is difficult to determine such a threshold. Theoretically, it is found that, when the defect gets deeper the propagation constant of the DM moves deeper, toward a higher band-gap. Because of the limited number of fully opened higher gaps, the propagation constant of the DM may move into a higher Bloch band and eventually localized DM disappears [41].

Finally, a DCV beam is used as a probe beam sent into the tunable negative defect to check whether a high-order optical vortex can be guided in it. We find the DCV cannot be guided and it tends to break up again into a quadruple-like structure when the defect strength is not too deep. Typical experimental results are shown in Figure 9. These results were obtained when the lattice spacing is 42 μm, the biased field is about 3.4 kV/cm, and the intensity ratio is $I_d/I_c = 2$. As before with nonlinear propagation of DCVs, the linear output is no longer in a donut shape, but rather turns into a quadrupole pattern with the symmetry similar to the lattice as shown in Figure 9(c). However, when the defect strength is very strong (i.e., intensity at the defect site is close to zero as in Figure 9(d)), even the quadrupole-like pattern cannot be maintained (Figure 9(e)). Under this condition, there is no light guided at the defect site at all when the bias field or the lattice intensity is increased.

5. Summary and Conclusions

We have studied experimentally the dynamical propagation of optical vortices in optically induced square photonic lattices under different settings. Inside the uniform photonic lattices, we find that the SCV beams self-trap into stable gap vortex solitons under four-site excitation with a defocusing nonlinearity. However, the DCV beams tend to break up and turn into quadrupole gap solitons. With geometrically extension eight-site excitation, the DCV beams can evolve into stable gap vortex solitons. Both the SCV and DCV gap solitons do not bifurcate from modes at the band edges, which is different from all the previously observed gap solitons. At the lattice surface, the SCV beams turn into stable surface vortex solitons in the semi-infinite gap under the four-site excitation with a self-focusing nonlinearity. However, they evolve into unstable quasivortex solitons with propagation constants in the first Bragg gap under the single-site excitation. In photonic lattices with negative defects, the SCV beams can be guided as linear vortex defect modes under appropriate defect conditions due to the bandgap guidance, while the DCV beams are unstable and evolve into quadrupole-like defect modes. Our results about such linear and nonlinear localized vortex states may prove to be relevant to similar vortex phenomena in other discrete systems beyond optics.

Acknowledgments

References

[1] A. S. Desyatnikov, Y. S. Kivhsar, and L. Torner, "Optical vortices and vortex solitons," in *Progress in Optics*, E. Wolf, Ed., vol. 47, pp. 219–319, North-Holland, Amsterdam ,The Netherlands, 2005.

[2] M. R. Dennis, Y. S. Kivshar, M. S. Soskin, and G. A. Swartzlander Jr., "Singular optics: more ado about nothing," *Journal of Optics A*, vol. 11, no. 9, Article ID 090201, 2009.

[3] G. A. Swartzlander and C. T. Law, "Optical vortex solitons observed in Kerr nonlinear media," *Physical Review Letters*, vol. 69, no. 17, pp. 2503–2506, 1992.

[4] J. Christou, V. Tikhonenko, Y. S. Kivshar, and B. Luther-Davies, "Vortex soliton motion and steering," *Optics Letters*, vol. 21, no. 20, pp. 1649–1651, 1996.

[5] G. Duree, M. Morin, G. Salamo et al., "Dark photorefractive spatial solitons and photorefractive vortex solitons," *Physical Review Letters*, vol. 74, no. 11, pp. 1978–1981, 1995.

[6] Z. Chen, M. Segev, D. W. Wilson, R. E. Muller, and P. D. Maker, "Self-trapping of an optical vortex by use of the bulk photovoltaic effect," *Physical Review Letters*, vol. 78, no. 15, pp. 2948–2951, 1997.

[7] Z. Chen, M. F. Shih, M. Segev, D. W. Wilson, R. E. Muller, and P. D. Maker, "Steady-state vortex-screening solitons formed in biased photorefractive media," *Optics Letters*, vol. 22, no. 23, pp. 1751–1753, 1997.

[8] Z. Chen, M. Mitchell, M. Segev, T. H. Coskun, and D. N. Christodoulides, "Self-trapping of dark incoherent light beams," *Science*, vol. 280, no. 5365, pp. 889–891, 1998.

[9] W. J. Firth and D. V. Skryabin, "Optical solitons carrying orbital angular momentum," *Physical Review Letters*, vol. 79, no. 13, pp. 2450–2453, 1997.

[10] C. C. Jeng, M. F. Shih, K. Motzek, and Y. Kivshar, "Partially incoherent optical vortices in self-focusing nonlinear media," *Physical Review Letters*, vol. 92, no. 4, pp. 439041–439044, 2004.

[11] I. Towers and B. A. Malomed, "Stable (2+1)-dimensional solitons in a layered medium with sign-alternating Kerr nonlinearity," *Journal of the Optical Society of America B*, vol. 19, no. 3, pp. 537–543, 2002.

[12] D. Briedis, D. E. Petersen, D. Edmundson, W. Krolikowski, and O. Bang, "Ring vortex solitons in nonlocal nonlinear media," *Optics Express*, vol. 13, no. 2, pp. 435–443, 2005.

[13] B. A. Malomed and P. G. Kevrekidis, "Discrete vortex solitons," *Physical Review E*, vol. 64, no. 2, pp. 266011–266016, 2001.

[14] J. Yang and Z. H. Musslimani, "Fundamental and vortex solitons in a two-dimensional optical lattice," *Optics Letters*, vol. 28, no. 21, pp. 2094–2096, 2003.

[15] D. N. Neshev, T. J. Alexander, E. A. Ostrovskaya et al., "Observation of discrete vortex solitons in optically induced photonic lattices," *Physical Review Letters*, vol. 92, no. 12, p. 123903, 2004.

[16] J. W. Fleischer, G. Bartal, O. Cohen et al., "Observation of vortex-ring "discrete" solitons in 2D photonic lattices," *Physical Review Letters*, vol. 92, no. 12, p. 123904, 2004.

[17] G. Bartal, O. Manela, O. Cohen, J. W. Fleischer, and M. Segev, "Observation of second-band vortex solitons in 2D photonic lattices," *Physical Review Letters*, vol. 95, no. 5, Article ID 053904, pp. 1–4, 2005.

[18] A. Bezryadina, E. Eugenieva, and Z. Chen, "Self-trapping and flipping of double-charged vortices in optically induced photonic lattices," *Optics Letters*, vol. 31, no. 16, pp. 2456–2458, 2006.

[19] B. Terhalle, D. Göries, T. Richter et al., "Anisotropy-controlled topological stability of discrete vortex solitons in optically induced photonic lattices," *Optics Letters*, vol. 35, no. 4, pp. 604–606, 2010.

[20] B. Terhalle, T. Richter, K. J. H. Law et al., "Observation of double-charge discrete vortex solitons in hexagonal photonic lattices," *Physical Review A*, vol. 79, no. 4, pp. 043821–043828, 2009.

[21] B. Terhalle, T. Richter, A. S. Desyatnikov et al., "Observation of multivortex solitons in photonic lattices," *Physical Review Letters*, vol. 101, no. 1, pp. 013903–013904, 2008.

[22] K. J. H. Law, A. Saxena, P. G. Kevrekidis, and A. R. Bishop, "Stable structures with high topological charge in nonlinear photonic quasicrystals," *Physical Review A*, vol. 82, no. 3, Article ID 035802, 2010.

[23] H. Martin, E. D. Eugenieva, Z. Chen, and D. N. Christodoulides, "Discrete solitons and soliton-induced dislocations in partially coherent photonic lattices," *Physical Review Letters*, vol. 92, no. 12, p. 123902, 2004.

[24] Z. Chen, H. Martin, E. D. Eugenieva, J. Xu, and A. Bezryadina, "Anisotropic enhancement of discrete diffraction and formation of two-dimensional discrete-soliton trains," *Physical Review Letters*, vol. 92, no. 14, p. 143902, 2004.

[25] N. K. Efremidis, J. Hudock, D. N. Christodoulides, J. W. Fleischer, O. Cohen, and M. Segev, "Two-dimensional optical lattice solitons," *Physical Review Letters*, vol. 91, no. 21, pp. 213906/1–213906/4, 2003.

[26] D. Song, C. Lou, L. Tang et al., "Self-trapping of optical vortices in waveguide lattices with a self-defocusing nonlinearity," *Optics Express*, vol. 16, no. 14, pp. 10110–10116, 2008.

[27] G. Bartal, O. Cohen, H. Buljan, J. W. Fleischer, O. Manela, and M. Segev, "Brillouin zone spectroscopy of nonlinear photonic lattices," *Physical Review Letters*, vol. 94, no. 16, Article ID 163902, 2005.

[28] C. Lou, X. Wang, J. Xu, Z. Chen, and J. Yang, "Nonlinear spectrum reshaping and gap-soliton-train trapping in optically induced photonic structures," *Physical Review Letters*, vol. 98, no. 21, Article ID 213903, 2007.

[29] L. Tang, C. Lou, X. Wang et al., "Observation of dipole-like gap solitons in self-defocusing waveguide lattices," *Optics Letters*, vol. 32, no. 20, pp. 3011–3013, 2007.

[30] J. Wang and J. Yang, "Families of vortex solitons in periodic media," *Physical Review A*, vol. 77, no. 3, Article ID 033834, 2008.

[31] K. J. H. Law, D. Song, P. G. Kevrekidis, J. Xu, and Z. Chen, "Geometric stabilization of extended S=2 vortices in two-dimensional photonic lattices: theoretical analysis, numerical computation, and experimental results," *Physical Review A*, vol. 80, no. 6, Article ID 063817, 2009.

[32] S. Suntsov, K. G. Makris, G. A. Siviloglou et al., "Observation of one- and two-dimensional discrete surface spatial solitons," *Journal of Nonlinear Optical Physics and Materials*, vol. 16, no. 4, pp. 401–426, 2007.

[33] H. Susanto, P. G. Kevrekidis, B. A. Malomed, R. Carretero-González, and D. J. Frantzeskakis, "Discrete surface solitons in two dimensions," *Physical Review E*, vol. 66, Article ID 046602,

2007.

[34] Y. V. Kartashov, A. A. Egorov, V. A. Vysloukh, and L. Torner, "Surface vortex solitons," *Optics Express*, vol. 14, no. 9, pp. 4049–4057, 2006.

[35] D. Song, C. Lou, K. J. H. Law et al., "Self-trapping of optical vortices at the surface of an induced semi-infinite photonic lattice," *Optics Express*, vol. 18, no. 6, pp. 5873–5878, 2010.

[36] S. Suntsov, K. G. Makris, D. N. Christodoulides et al., "Observation of discrete surface solitons," *Physical Review Letters*, vol. 96, no. 6, Article ID 063901, 2005.

[37] X. Wang, A. Bezryadina, Z. Chen, K. G. Makris, D. N. Christodoulides, and G. I. Stegeman, "Observation of two-dimensional surface solitons," *Physical Review Letters*, vol. 98, no. 12, Article ID 123903, 2007.

[38] I. Makasyuk, Z. Chen, and J. Yang, "Band-gap guidance in optically induced photonic lattices with a negative defect," *Physical Review Letters*, vol. 96, no. 22, Article ID 223903, 2006.

[39] A. Szameit, Y. V. Kartashov, M. Heinrich et al., "Observation of two-dimensional defect surface solitons," *Optics Letters*, vol. 34, no. 6, pp. 797–799, 2009.

[40] J. Wang, J. Yang, and Z. Chen, "Two-dimensional defect modes in optically induced photonic lattices," *Physical Review A*, vol. 76, no. 1, Article ID 013828, 2007.

[41] D. Song, X. Wang, D. Shuldman et al., "Observation of bandgap guidance of optical vortices in a tunable negative defect," *Optics Letters*, vol. 35, no. 12, pp. 2106–2108, 2010.

Composition Comments

1. We dehyphenated the highlighted part in the main title as per journal style. Please check.

2. There is a difference between the manuscript and the new electronic version in Figure 6(a) and we followed the new electronic version. Please check.

3. Comment on ref. [6]: We split this reference to [6, 7]. Please check.

Author(s) Name(s)

It is very important to confirm the author(s) first and last names in order to be displayed correctly on our website as well as in the indexing databases:

Author 1

Last Name: Song

First Name: Daohong

Author 2

Last Name: Lou

First Name: Cibo

Author 3

Last Name: Tang

First Name: Liqin

Author 4

Last Name: Ye

First Name: Zhuoyi

Author 5

Last Name: Xu

First Name: Jingjun

Author 6

Last Name: Chen

First Name: Zhigang